Study of light Sn isotopes through Coulomb excitation and (d,p) transfer experiments

Joochun (Jason) Park

Center for Exotic Nuclear Studies, IBS

Canada-APCTP Meeting on Nuclear Theory

Aug. 11, 2022

Main theme: structure of ^{100}Sn and neighboring isotopes

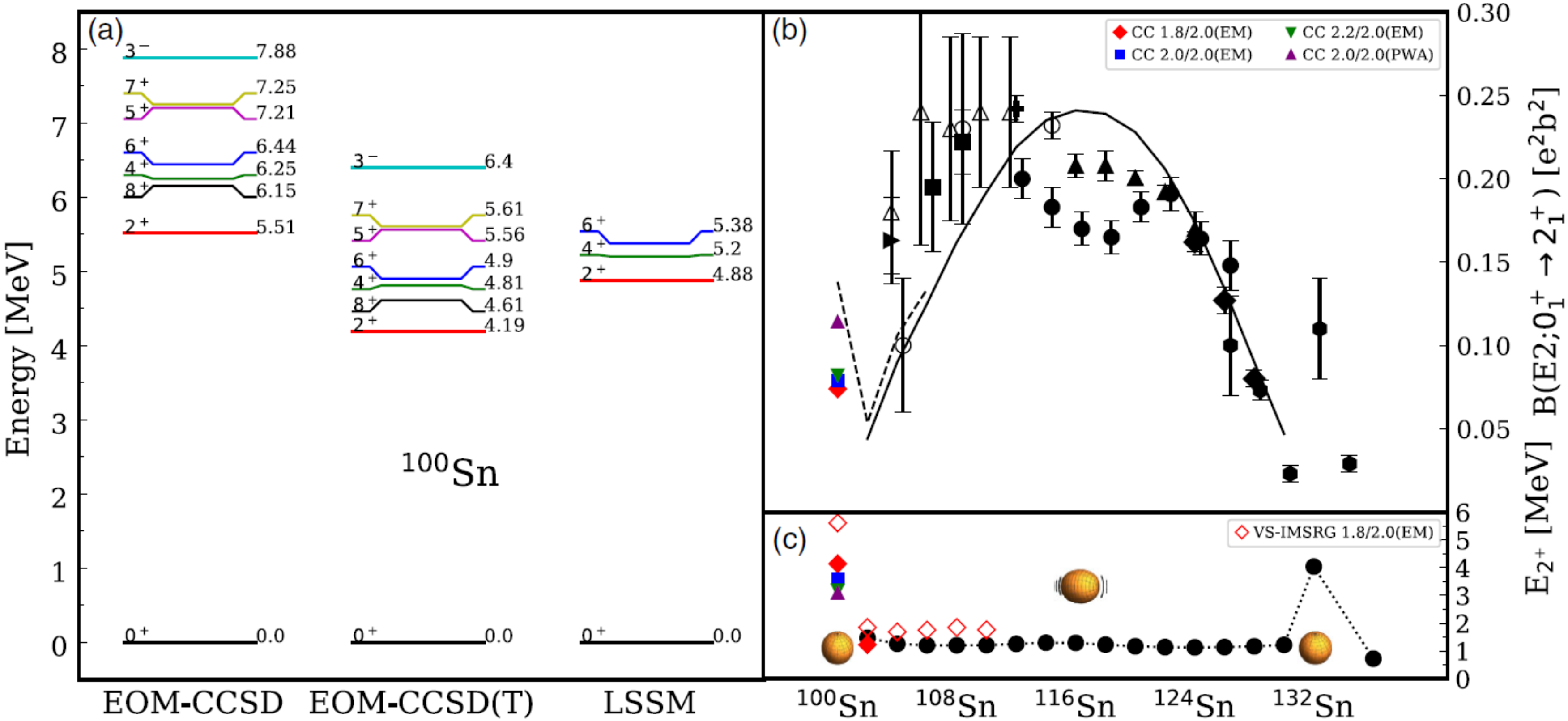

T. D. Morris et al., PRL 120, 152503 (2018)

Spectroscopy around ^{100}Sn: tests of microscopic models to describe:

- Single-particle energies and spectroscopic factors
- Shell robustness and evolution
- Core excitation and polarization
- *pn* interaction

Experimental methods along light Sn isotopes:

- **Coulomb excitation**
- Nucleon knockout
- Fusion evaporation
- Total absorption spectroscopy
- **Transfer/pickup reactions**

I. Collectivity and shapes of even-*A* Sn isotopes

Structural evolution in Sn isotopes

Sn (Z = 50) isotopic chain ideal for studies on shell evolution, spanning N = 50-82 and beyond

Many B(E2) measurements appear enhanced towards neutron-deficient ^{100}Sn

Dynamic changes in shapes of excited states as a possible explanation ^{110}Sn (N = 60), driven by proton excitations across $g_{9/2}$ orbital

Framework: Monte Carlo Shell Model

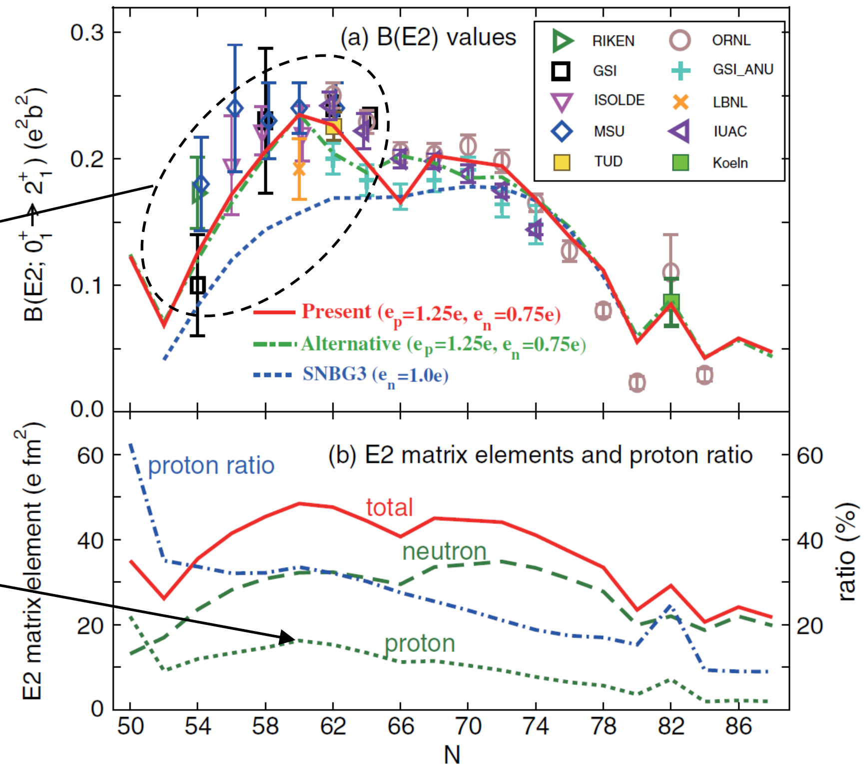

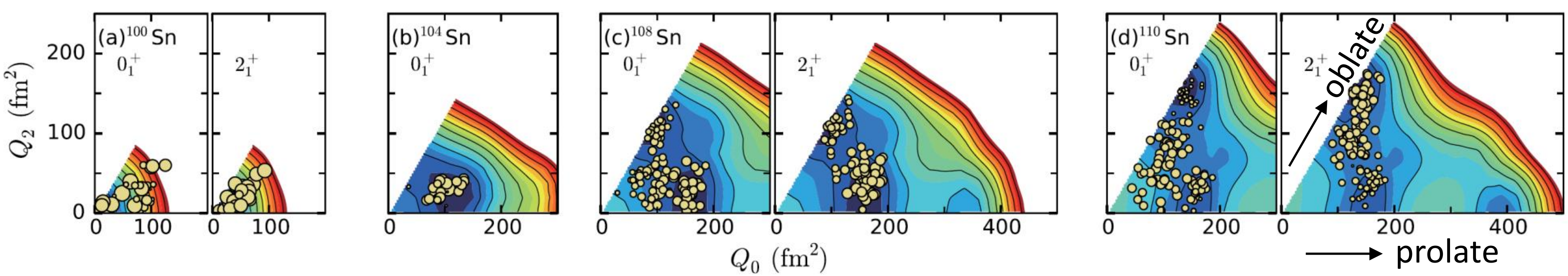

T. Togashi *et al.*, PRL **121**, 062501 (2018)

Recent/ongoing B(E2) measurements in the light Sn region

Intermediate-energy Coulomb excitation of ^{102}Sn and ^{100}Cd at RIBF in 2019

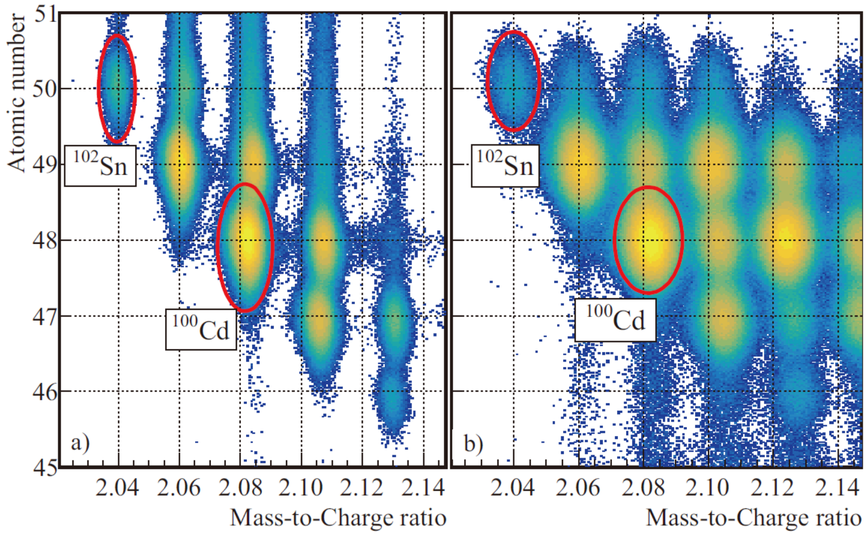

M. L. Cortes et al., RIKEN APR 53, 36 (2020)

Also first attempt at in-beam gamma-ray spectroscopy of ^{100}Sn with DALI2 (NaI detector array)

S. Chen et al., RIKEN APR 53, 35 (2020)

Lifetime measurements of states in ^{106,108}Sn with deep inelastic scattering + plunger method at GANIL

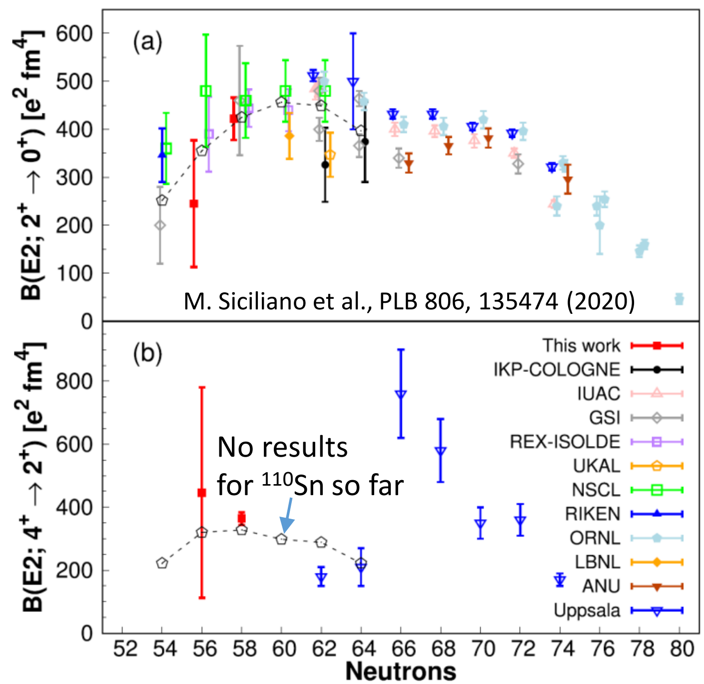

B(E2) measurements of higher-lying states Initiated

Uncertainties still large for light Sn (A < 112)

Principles of Coulomb excitation

<u>Main purpose:</u> B(E2), B(E3), Q_2, Q_3 measurements related to collectivity and deformation in nuclear structure

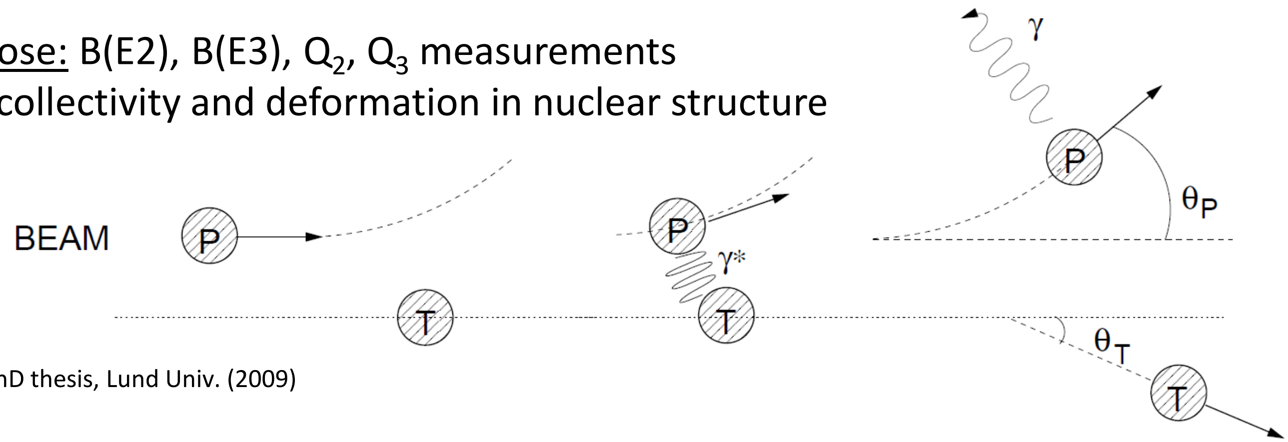

A. Ekström, PhD thesis, Lund Univ. (2009)

- Electromagnetic excitation between projectile (beam) and target nucleus through Coulomb field
- Detection of γ rays and Doppler correction using kinematics ($\beta = v/c$), θ_γ, θ_p and θ_t
- Nuclear excitation can be separated from pure electromagnetic interaction at "safe" Coulex energy:

$$E_{\text{safe}} = 1.44 \frac{A_p + A_t}{A_t} \frac{Z_p \cdot Z_t}{1.25(A_p^{1/3} + A_t^{1/3}) + 5} \text{MeV}$$

K. Alder and A. Winther, *Electromagnetic Excitation* (1975)

Coulex experiments performed at HIE-ISOLDE using ^{206}Pb target ($Z_t = 82$, $A_t = 206$)

Z_p	A_p	E_{safe} (MeV)	E_{safe}/A_p (MeV)	E_{exp}/A_p (MeV), year
50	110	493	4.48	4.40 (2016)
50	108	491	4.54	4.50 (2017)
50	106	489	4.61	4.40 (2018)

Radioactive ^{106,108,110}Sn beam production at CERN HIE-ISOLDE

RIB production from spallation of 1.4-GeV protons from PS booster on LaC_x target
Isobaric contamination (^{106,108,110}In) suppressed with Resonance Ionization Laser Ion Source (RILIS)

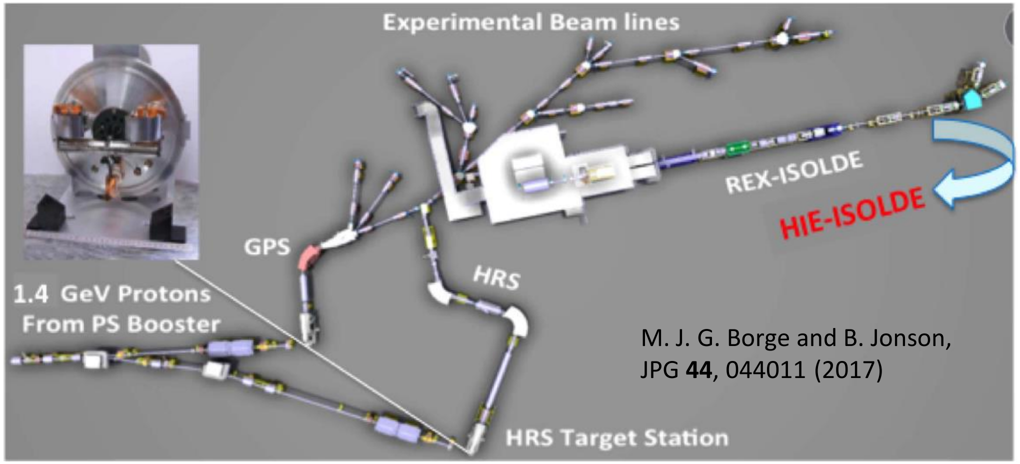

Post-accelerated beam through HRS to HIE-ISOLDE,
towards Miniball among multiple experiment stations

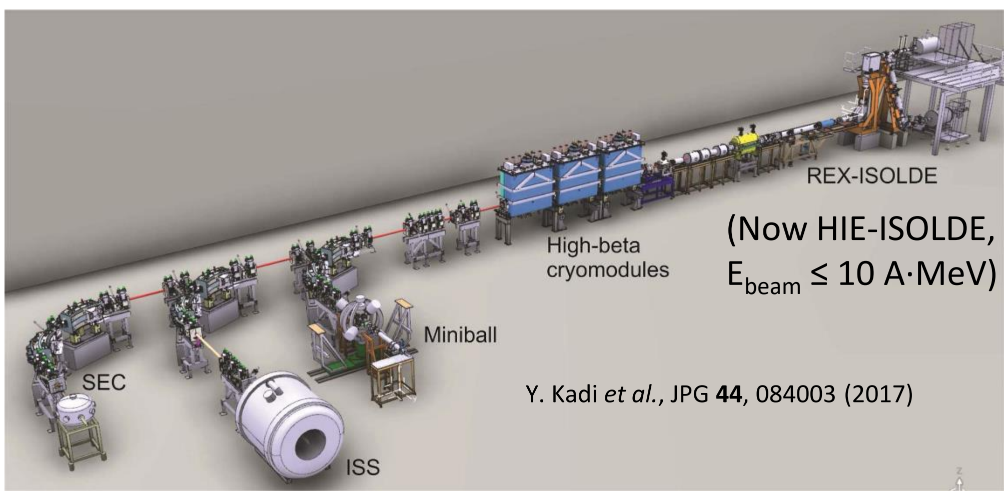

Coulex with Miniball at HIE-ISOLDE

Segmented HPGe detectors for Doppler correction following Coulex or transfer reaction

8 clusters x 3 crystals x 6 segments = 144 unique γ-ray detection angles

$2.0\text{-}4.0\ \mathrm{mg/cm^2}$ secondary targets, minor beam energy loss through target

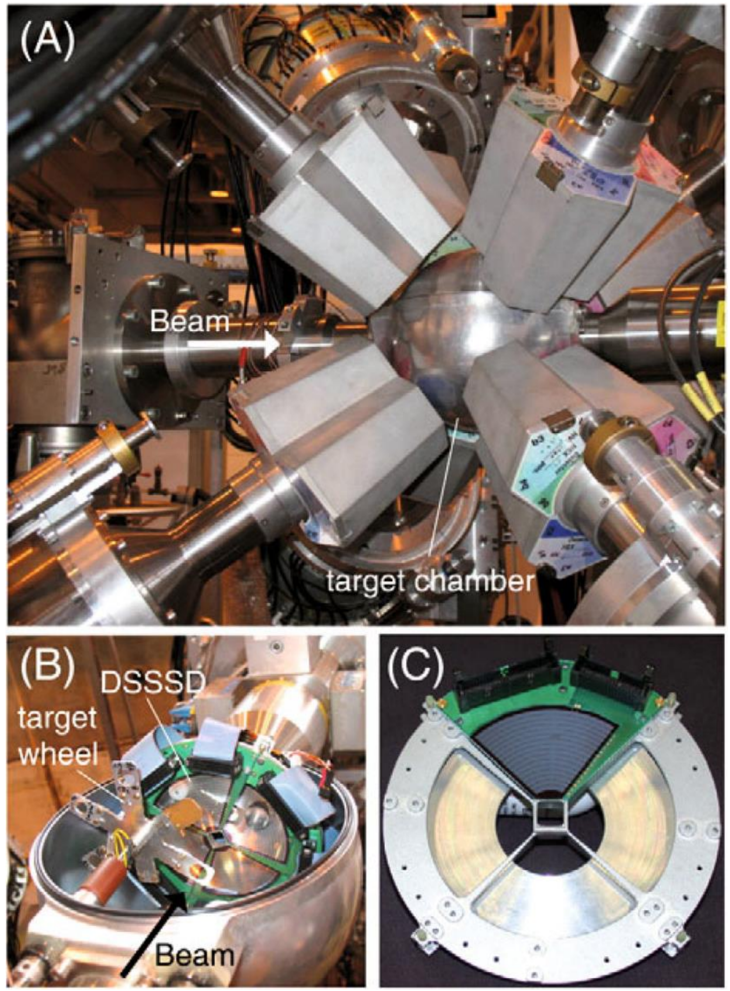

N. Warr *et al.*, EPJA **49**, 40 (2013)

Highlight achievement:
evidence for octupole deformation

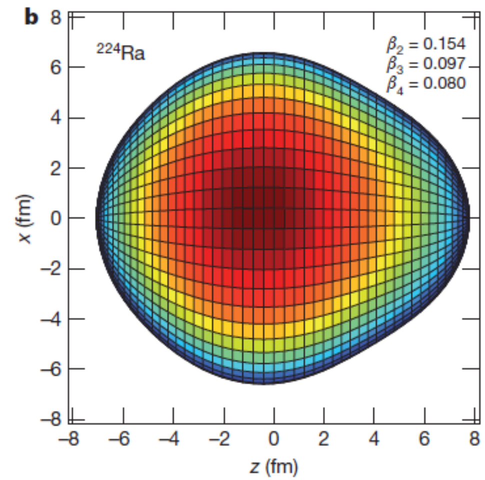

L. P. Gaffney *et al.*, Nature **497**, 199 (2013)

4-quadrant DSSSD with 16 rings x 16 sectors for particle ID and angles, thickness ~500 µm

Preliminary results on ^{106,108,110}Sn

Substantial statistics for γ-ray peaks with high-*Z* target:

- Improved precision on Coulex cross section/B(E2)
- New B(E2) values from higher states
- New excited states revealed through Coulex

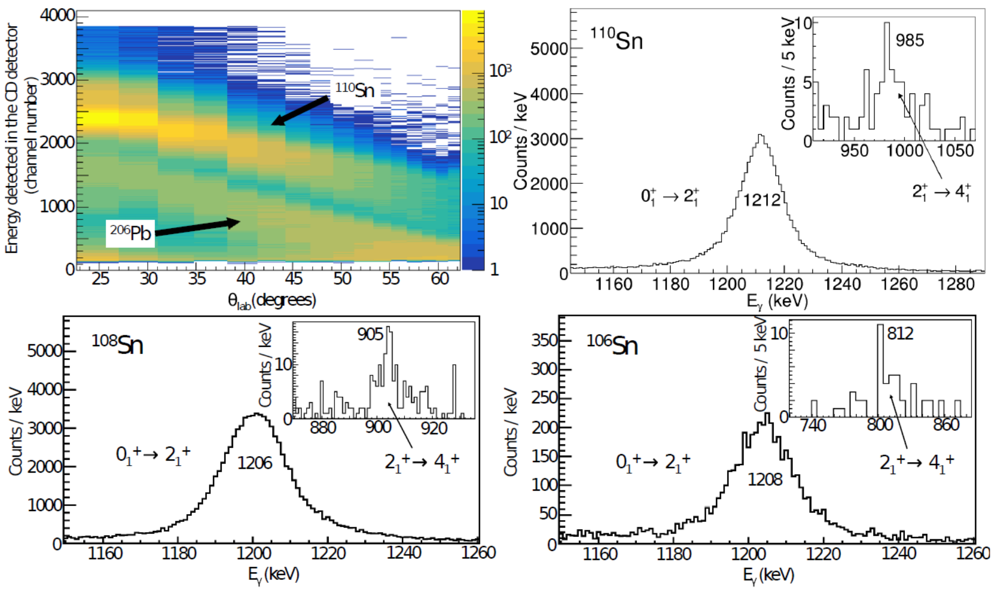

JP *et al.*, JPS Conf. Proc. **32**, 010036 (2020)

Much more γγ coincidences for ^{108}Sn compared to ^{110}Sn – subject for further analysis

γ-γ coincidences for higher excited states

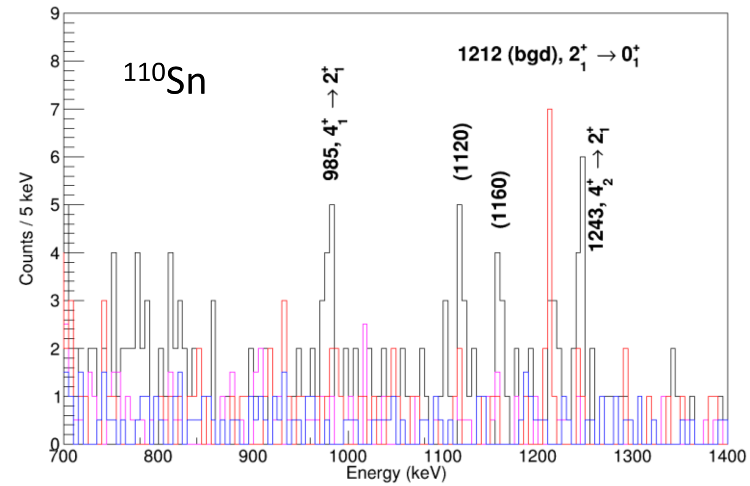

Gated on 1206(black)/905(red)-keV gammas

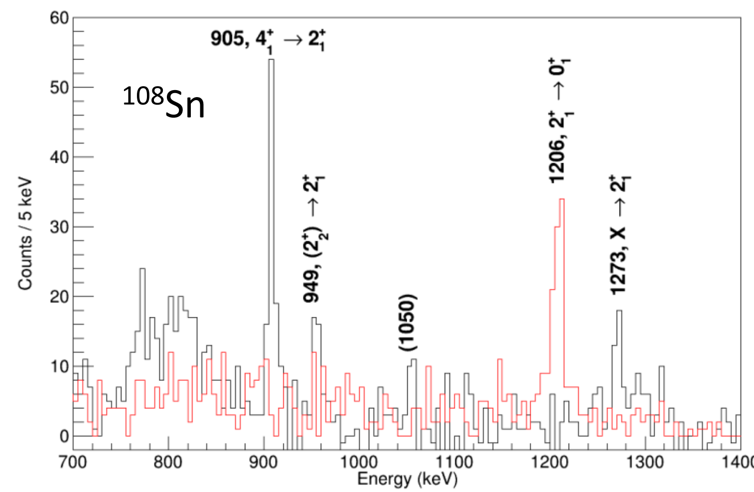

Lifetime measurements, B(E2) and Q_2

B(E1, E2, E3, M1, M2, etc…) values obtainable through the following:

γ-ray energy

γ-ray branching ratio

$$B(\sigma L) = \frac{1}{2J_i+1}\left|J_i\|\widehat{M}(\sigma L)\|J_f\right|^2 = K(\sigma L)E_\gamma^{-(2L+1)}\left(\frac{\ln(2)}{T_{1/2}}\right)\left(\frac{b}{1+\alpha}\right)$$

L-dependent factor (constants)

$$K(\sigma L) = \frac{(\hbar c)^{2L+1}L[(2L+1)!!]^2\hbar}{8\pi(L+1)}$$

Half-life $T_{1/2}$ (lifetime τ)

Internal conversion coefficient

Ex) $\tau^{-1} = 1.22\times E_\gamma^5 B(E2, J_i\to J_f)$ for E2 transition

$[\tau \text{ in ns}, E_\gamma \text{ in MeV}, B(EL) \text{ in } e^2\text{fm}^{2L}]$

Coulomb excitation cross section depends on Z_{targ}, E_{beam}, B(E2) and spectroscopic quadrupole moment $Q(2^+)$

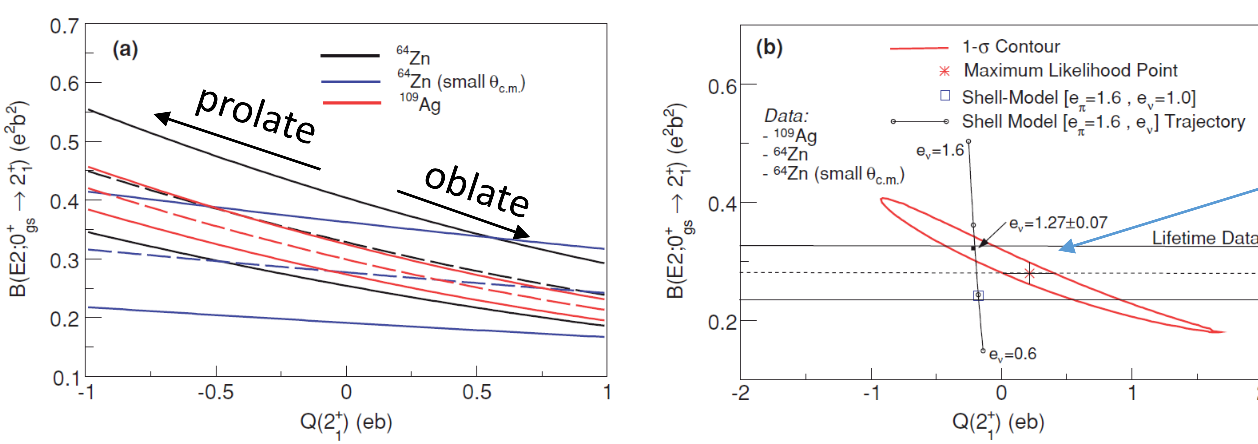

A. Ekström *et al.*, PRC **80**, 054302 (2009)

B(E2), $Q(2^+)$ from Coulex can be constrained by lifetime data, or alternative target/energies

Measuring the 2_1^+ state lifetime in ^{110}Sn with simulation

Geant4 simulation of Miniball + CD detector

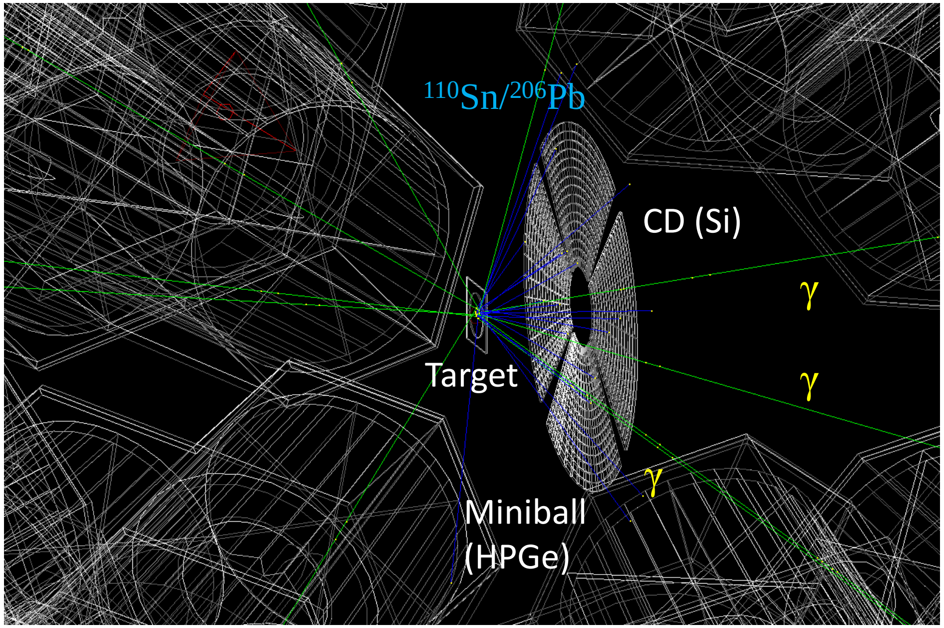

Method:

1. Replicate experimental conditions:
   - Geometry
   - Beam setting
   - Detector performance
2. Simulate particle kinematics and Doppler-shifted γ-ray events, employing different input lifetimes
3. Compare outputs with data and quote the lifetime with the best-matching result

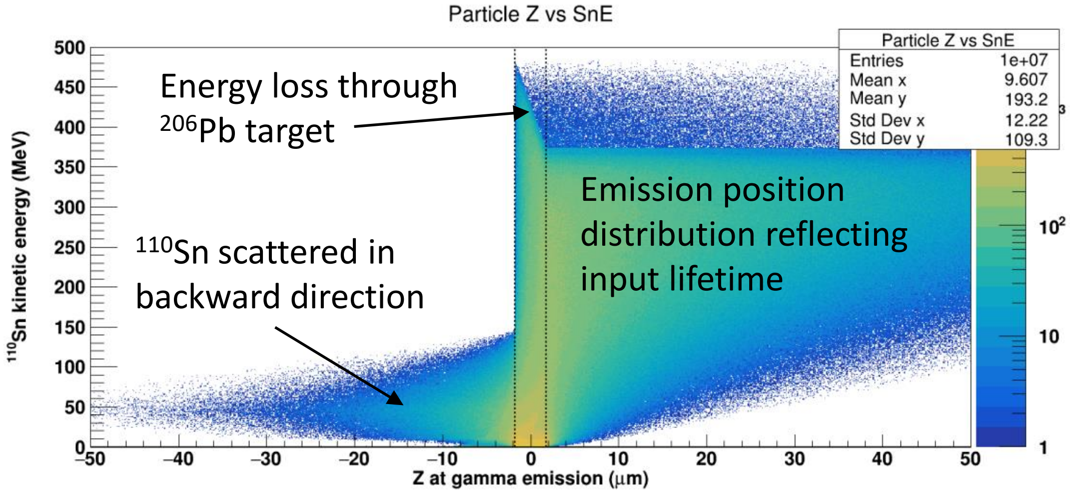

Lifetime analysis of the 2_1^+ state in ^{110}Sn

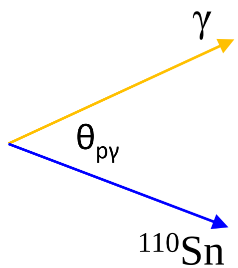

$$E_\gamma = E_0 \frac{\sqrt{1-\beta^2}}{1-\beta\cos\theta}$$

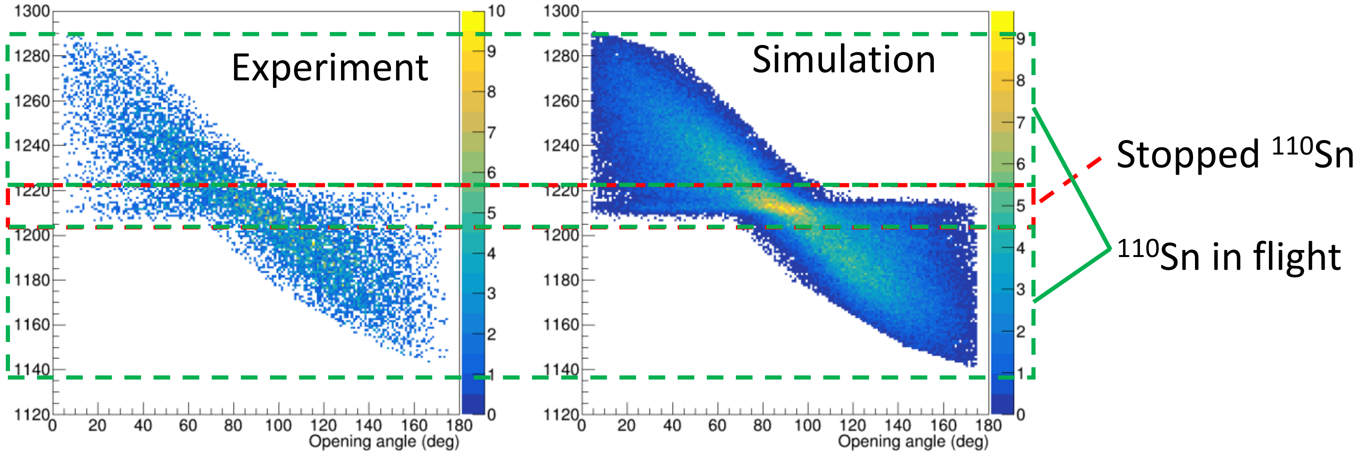

χ^2 minimization along a range of trial τ

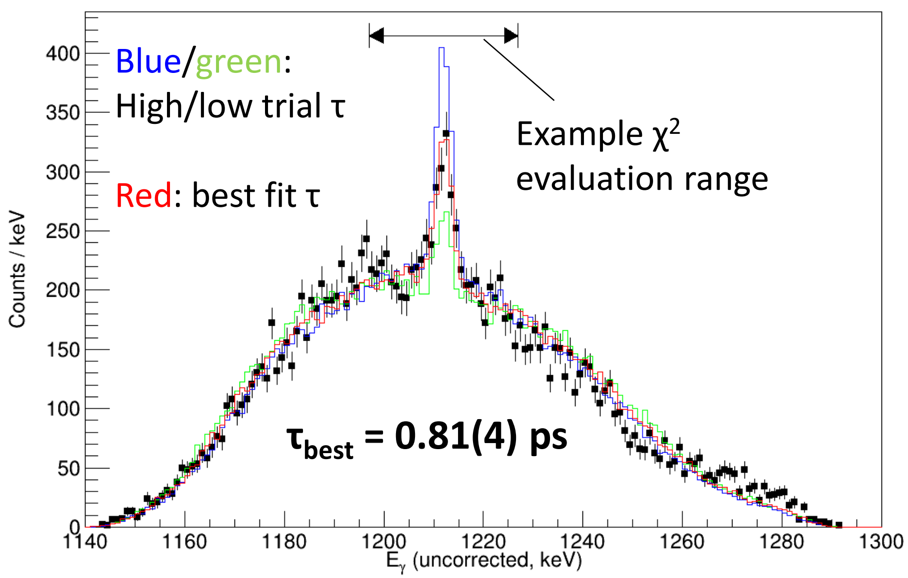

Feeding from long-lived 4^+ included

Previous measurement: τ = 0.81(10) ps with ^{12}C(^{106}Cd,^{8}Be)^{110}Sn reaction and lineshape analysis

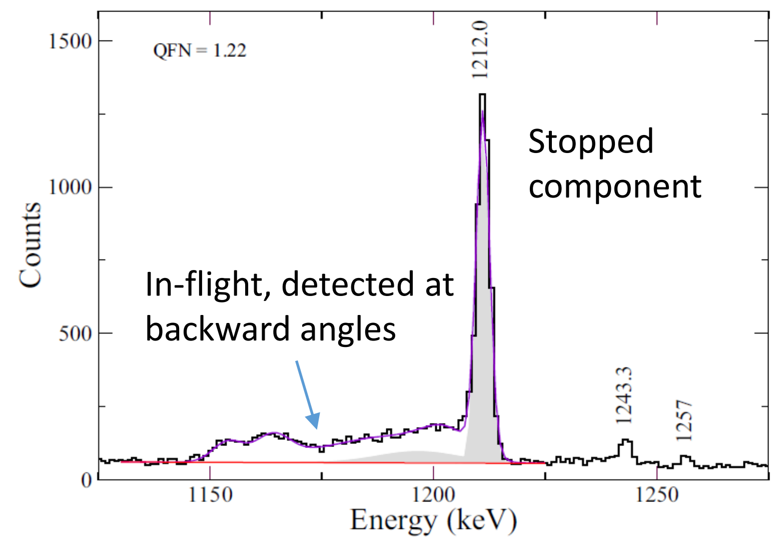

G. J. Kumbartzki *et al.*, PRC **93**, 044316 (2016)

B(E2) vs Q(2$^+$) state

B(E2) from lifetime measurement lower than B(E2) from Coulex assuming Q(2$^+$) = 0; consistency achieved if the 2$^+$ state is oblate deformed

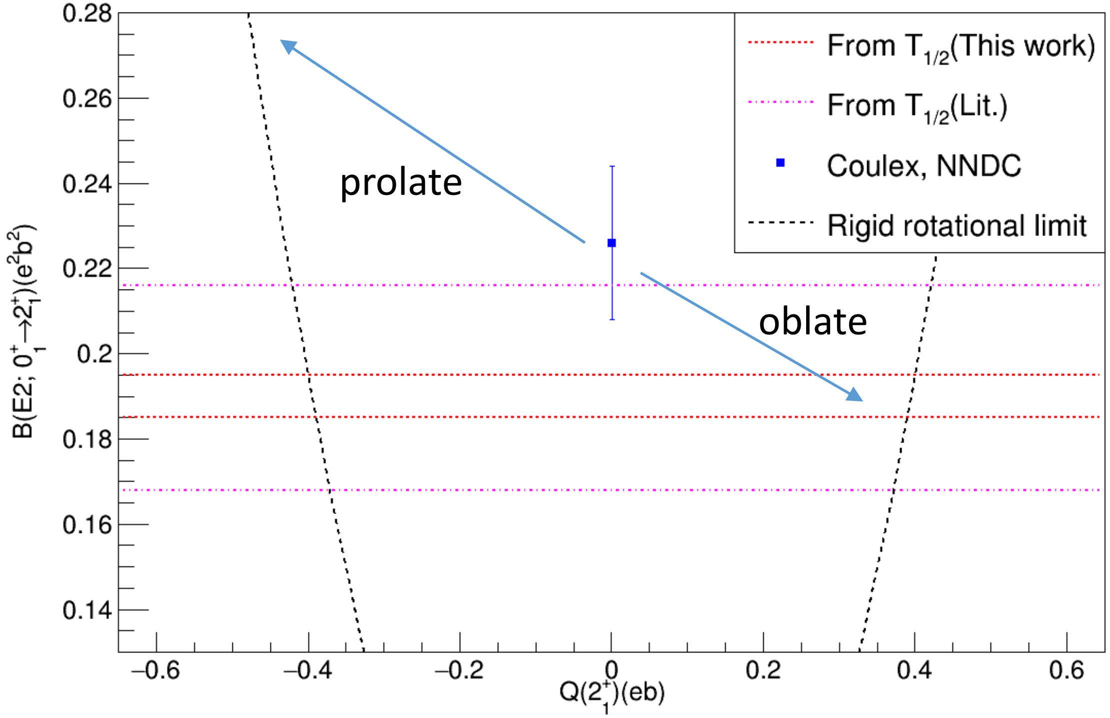

Excerpt from the MCSM paper:

As the $1g_{7/2}$ and $2d_{5/2}$ orbits are more filled, the T-plot extends farthest in ^{110}Sn [panel (d)] with the maximum calculated $B(E2)$ [see Fig. 2 (a)], while the tendency is changed from the prolate to the oblate shape.

T. Togashi *et al.*, PRL **121**, 062501 (2018)

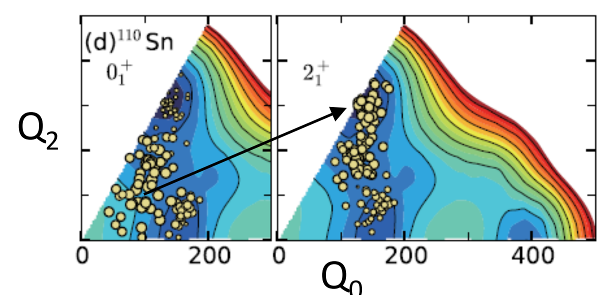

Subject of further discussion

Summary from the Coulex campaign IS562

Electromagnetic transition strengths in light Sn isotopes

- B(E2) values typically greater than predicted at low mass region; enhanced collectivity?

Coulomb excitation experiment with Miniball at HIE-ISOLDE

- Ideal target and safe Coulex beam energy to avoid nuclear effects
- High-statistics γ-ray data for precise cross sections and new B(E2) values of higher states
- Preliminary results in $^{106,108,110}Sn$ promising

Lifetime analysis of the 2_1^+ state in ^{110}Sn

- Geant4 simulation studies near completion
- Independent B(E2) and Q_2 values for comparisons with theory consistent with oblate deformation for the 2_1^+ state, traditionally assumed to be spherical!

IS562 experiment campaign collaborators:

J. Park[1], A. Knyazev[1], E. Rickert[1], P. Golubev[1], J. Cederkäll[1,2], A. N. Andreyev[2,3], G. de Angelis[4], K. Arnswald[5], L. Barber[6], C. Berger[7], C. Berner[7], T. Berry[8], M. J. G. Borge[2,9], A. Boukhari[2,10], D. Cox[11], J. Cubiss[3] D. M. Cullen[6], J. Díaz Ovejas[9], C. Fahlander[1], L. P. Gaffney[2], A. Gawlik[2,12], R. Gernhäuser[7], A. Görgen[13], T. Habermann[14], C. Henrich[14], A. Illana[15], J. Iwanicki[12], T. W. Johansen[13], J. Konki[2], T. Kröll[14], B. S. Nara Singh[16], G. Rainovski[17], C. Raison[3], P. Reiter[5], D. Rosiak[5], S. Saha[18], M. Saxena[12], M. Schilling[14], M. Seidlitz[14], J. Snäll[1], C. Stahl[14], M. Stryjczyk[19], O. Tengblad[9], G. M. Tveten[13], J. J. Valiente-Dobón[15], P. Van Duppen[19], S. Viñals[9], N. Warr[5], A. Welker[2], L. Werner[7], H. De Witte[19] and R. Zidarova[17]

II. Single-particle structure of odd-*A* Sn isotopes

Shell evolution in the light Sn isotopic chain

Spherical self-consistent HFB calculations with Z = 50

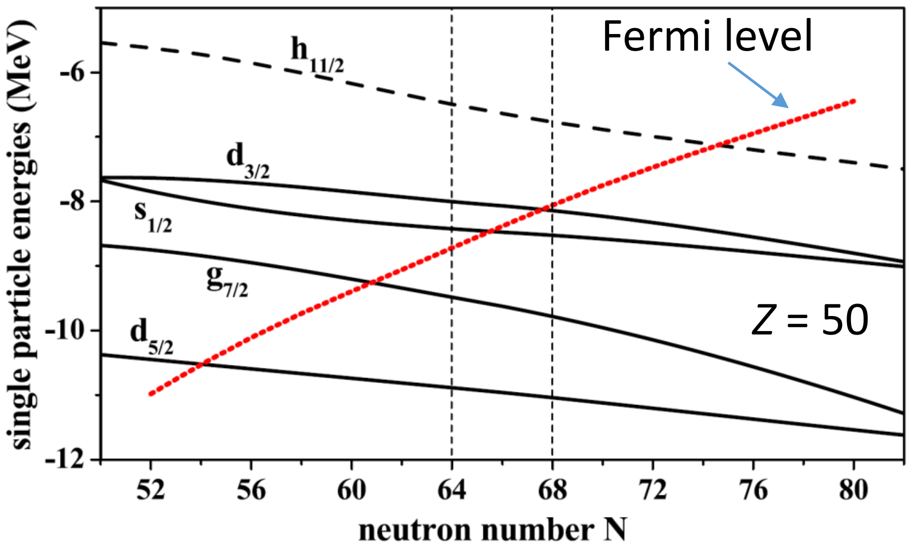

A. Jungclaus et al., PLB 695, 110 (2011)

Inclusion of 3N forces in recent theoretical developments

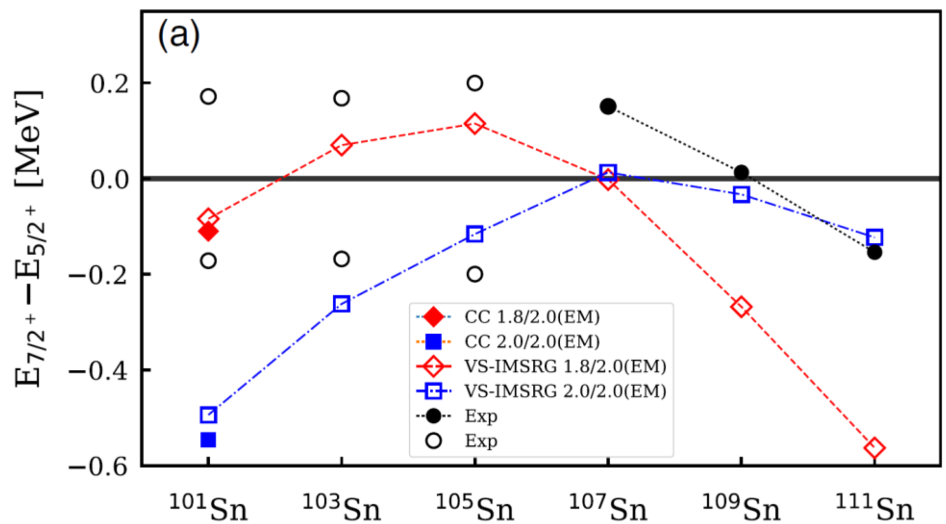

T. D. Morris et al., PRL 120, 152503 (2018)

Experimental literature on odd-mass, *A* < 112 Sn:

- Decay spectroscopy
- Fusion evaporation
- α-transfer reactions on Cd isotopes
- Pickup reactions

(d,p) spectroscopic factors unknown for *A* < 111 Sn isotopes

Ground-state spin assignments <u>still tentative</u> for ^{101,103,105}Sn

Tensor force to explain lowering of neutron $g_{7/2}$ relative to $d_{5/2}$ orbital

[T. Otsuka et al., PRL 95, 232502 (2005) and PRL 104, 012501 (2010)]

Single-particle state candidates and energy trends in $^{105\text{-}113}Sn$

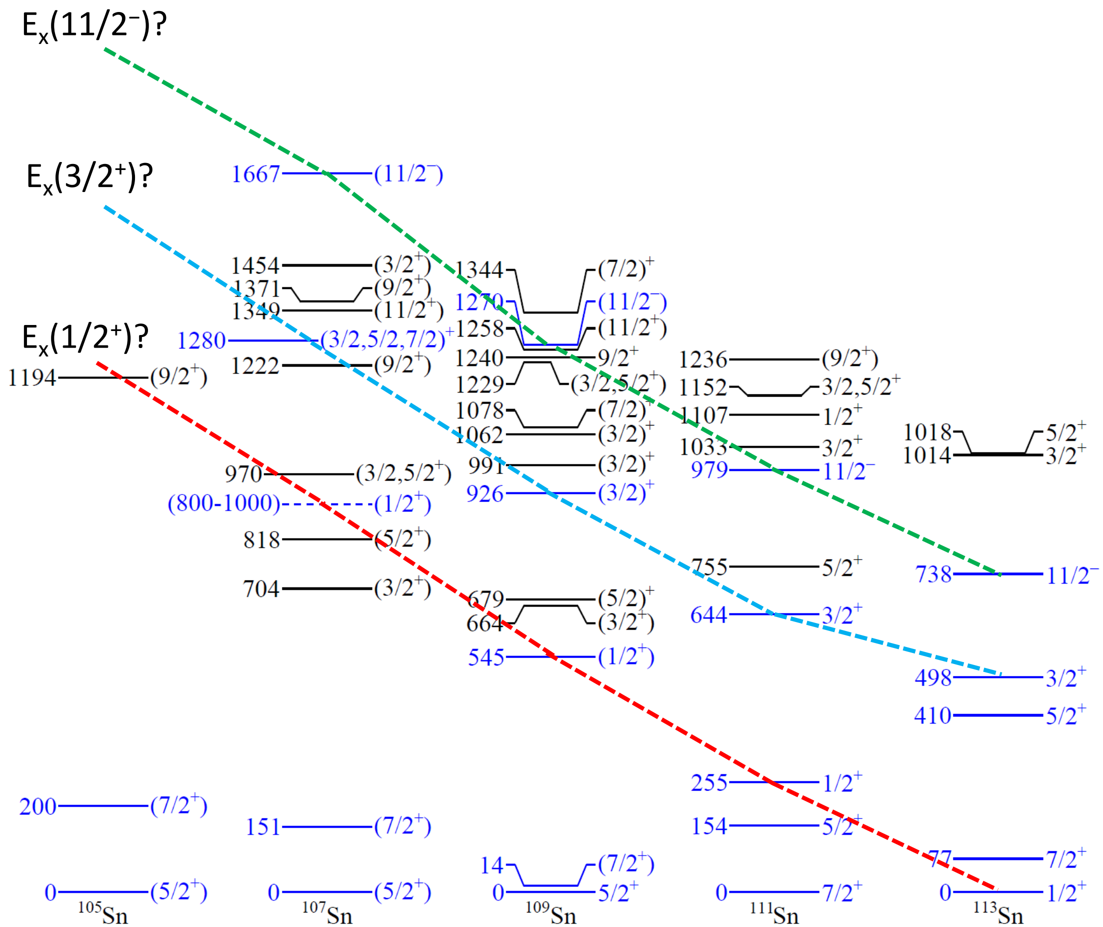

Tentative spin assignments based on beta-decay studies with γγ coincidences

Previously suggested single-particle states in blue, to be clearly determined through (d,p)

Energy of the unknown $1/2^+$ state in ^{107}Sn and identification of $11/2^-$ states (intruder orbit) particularly interesting, in addition to the S-factors

Aim of the proposal with the ISS

Historical (d,p), (d,t) reactions on stable Sn targets in normal kinematics, E_{beam} ~ 15 MeV/u:

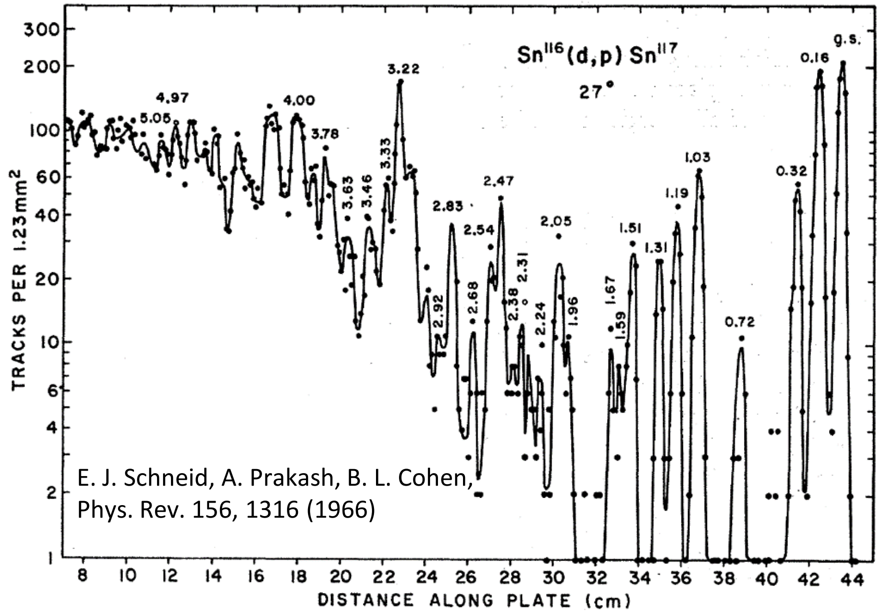

Transfer reactions with inverse kinematics with <u>light unstable Sn beams</u> on deuterated target

From 1n transfer reactions on even-mass Sn isotopes with ISS, we want to measure:
1. Energies and angular distributions of protons
→ Angular momentum transfer for J^{π} assignments of individual excited states
→ New states for further investigation of single-particle states

2. Transfer cross sections
→ Spectroscopic factors *S* for neutron occupation in *gdsh* orbitals above *N* = 50

ISS spectrometer for (d,p) in inverse kinematics

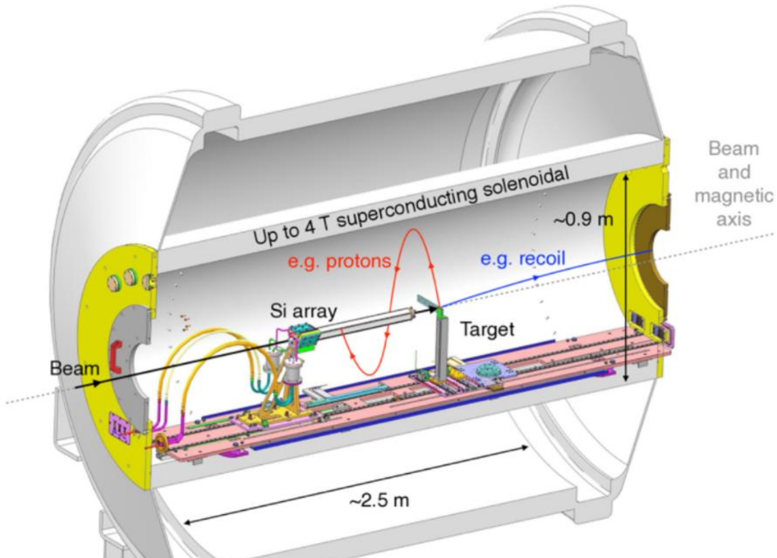

Taken from D. K. Sharp, NuSpin 2019

Proposed B-field strength: 2.5 T

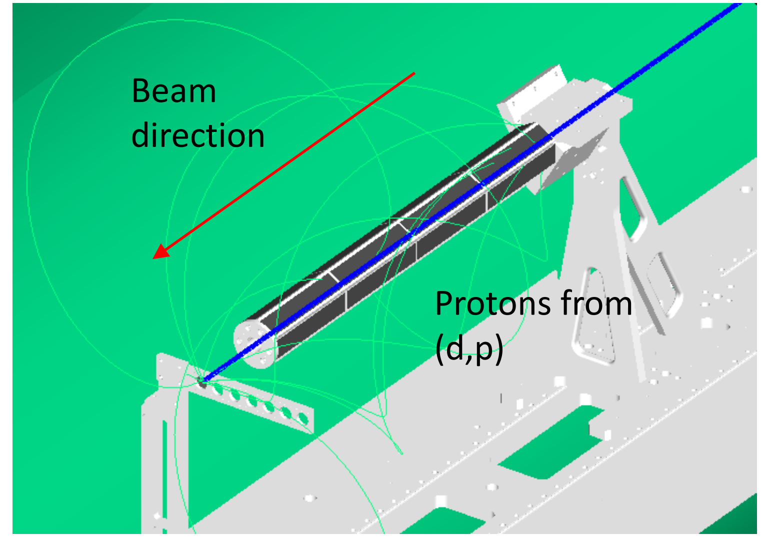

1-mm thick DSSDs arranged in hexagonal tube

94% Si strip/70% ϕ coverage

z-coverage: (-61.05 cm, -10.0 cm) from the target

At E_{beam} = 8 MeV/u, covers 8° < $\theta_{c.m.}$ < 49°

NPTool simulation of ISS

A. Matta et al. J. Phys. G 43, 045113 (2016) and M. Labiche

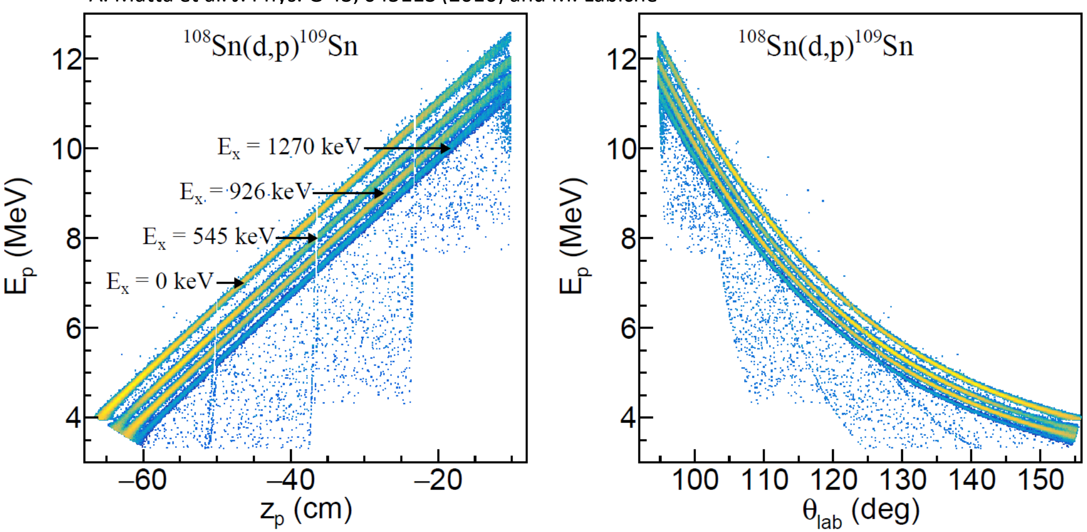

~100-keV FWHM resolution based on:

- $\Delta E_{beam} \leq 0.5\%$ FWHM
- 2-mm beam size for ^{28}Mg and ^{206}Hg
- 165-μg/cm^2 CD_2 target thickness, same as for ^{206}Hg experiment

ISOLDE Solenoidal Spectrometer

(d,p) cross section calculations with DWBA, through FRESCO

Relevant neutron orbitals above N = 50: $1g_{7/2}$, $2d_{5/2}$, $2d_{3/2}$, $3s_{1/2}$, $1h_{11/2}$

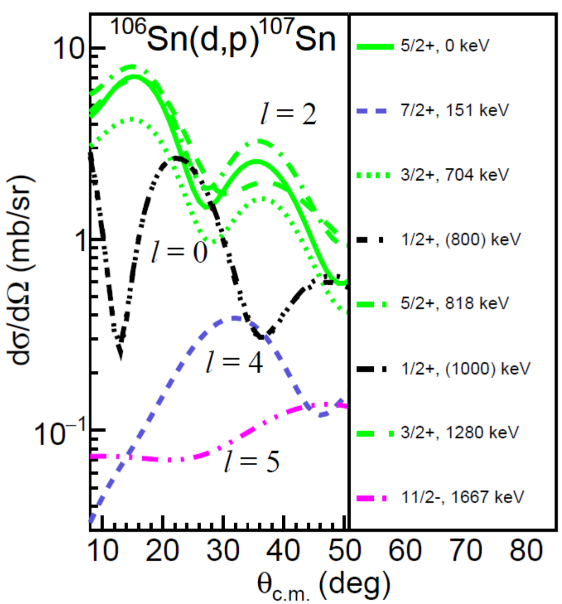

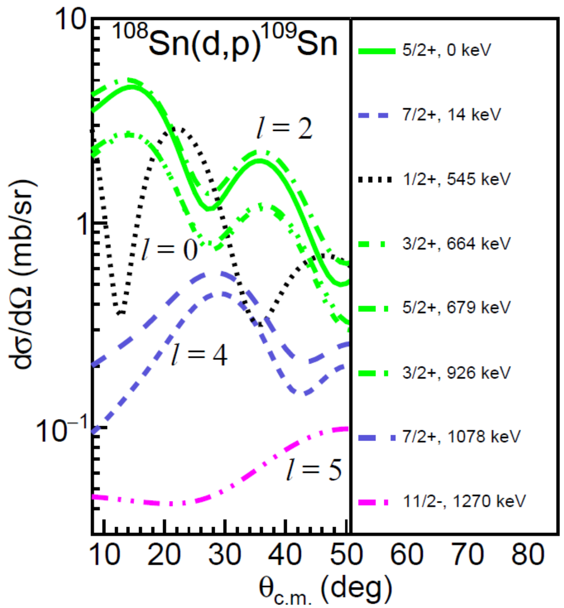

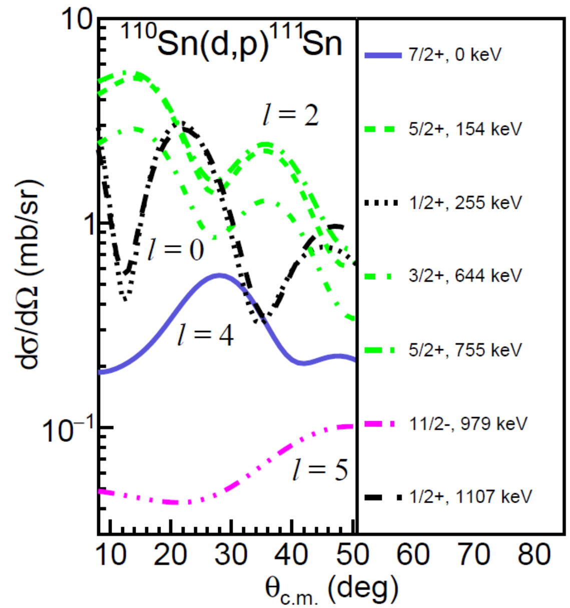

Entrance channel parameters:
H. An and C. Cai, PRC 73, 054605 (2006)

Exit channel parameters:
A.J. Koning and J.P. Delaroche, NPA 713, 231 (2003)

Automatic binding potential depth adjustment
I. Thompson, Compt. Phys. Rep. 7, 167 (1988)

Priority on measuring l = 5 transfers to $11/2^-$ states with sufficient statistics

Angular distribution trends well separated as a function of l for spin assignments

Beam time requests and expected statistics/spectra

Reaction/ target	Intensity and beam time	E_x (keV)	J^π	ΔL	σ (mb)	Proton counts
^{106}Sn$(d,p)^{107}$Sn at 8 MeV/u on 165-μg/cm^2 CD$_2$	1×10^5/s for 24 shifts	0	$5/2^+$	2	4.436	1378
		151	$(7/2^+)$	4	0.461	143
		704	$(3/2^+)$	2	3.444	1070
		818	$(5/2^+)$	2	6.576	2043
		(800-1000)	$(1/2^+)$	0	2.031-2.072	631-644
		1280	$(3/2^+)$	2	5.641	1753
		1667	$(11/2^-)$	5	0.220	68
^{108}Sn$(d,p)^{109}$Sn at 8 MeV/u on 165-μg/cm^2 CD$_2$	5×10^5/s for 12 shifts	0	$5/2^+$	2	3.893	3018
		14	$(7/2^+)$	4	0.547	424
		545	$(1/2^+)$	0	2.220	1722
		664	$(3/2^+)$	2	2.357	1828
		679	$(5/2^+)$	2	2.411	1869
		926	$(3/2^+)$	2	2.463	1910
		1078	$(7/2^+)$	4	0.750	581
		1270	$(11/2^-)$	5	0.141	109
^{110}Sn$(d,p)^{111}$Sn at 8 MeV/u on 165-μg/cm^2 CD$_2$	5×10^5/s for 12 shifts	0	$7/2^+$	4	0.685	532
		154	$5/2^+$	2	4.378	3401
		255	$1/2^+$	0	2.346	1822
		644	$3/2^+$	2	2.553	1983
		755	$5/2^+$	2	4.813	3738
		979	$11/2^-$	5	0.147	114
		1107	$1/2^+$	0	2.458	1909

Transfer reaction quenching by 0.55 applied
[B. P. Kay, J. P. Shiffer, S. J. Freeman, PRL 111, 042502 (2013)]

Statistics comparable to d(^{206}Hg,p)^{207}Hg results

Beam time set to measure transfers to $11/2^-$ states with ~10^2 counts at nominal RIB intensities, updated cross sections and lower E_{beam} can improve these numbers by 70-100%

Search for $1/2^+$ single-particle state in ^{107}Sn in E_x range 800-1000 keV with little dependence on cross section

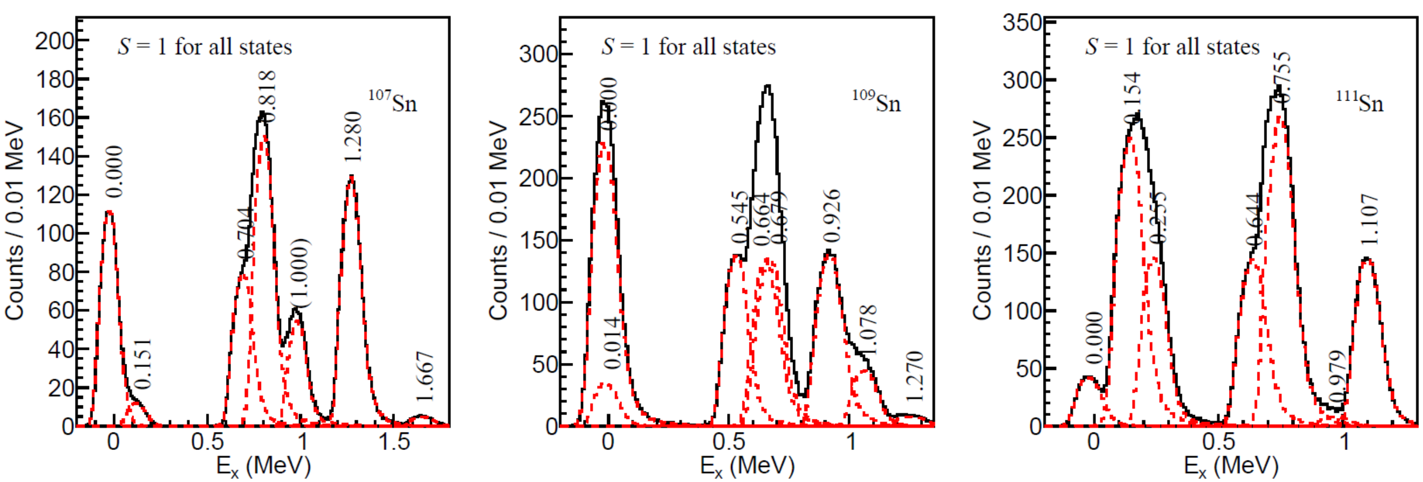

ISS spectra from potential In (Z = 49) contaminant

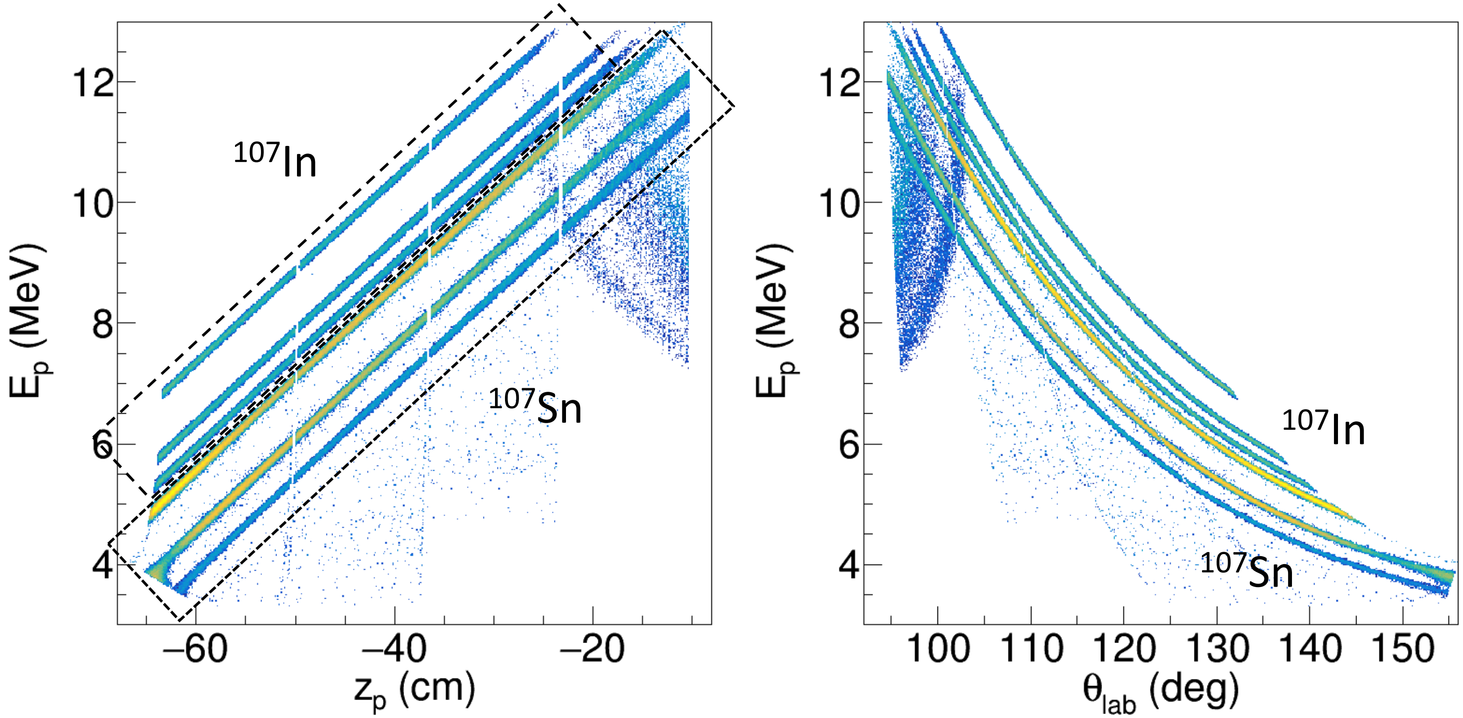

If reconstructing only on protons (no recoil detection) with isobars, reaction kinematics simply governed by

$Q_x = Q_{g.s.} - E_x$

A	**$Q_{g.s.}$(Sn), MeV**	**$Q_{g.s.}$(In), MeV**	**ΔQ(In-Sn)**
106	7.00	8.80	1.80
108	6.41	8.22	1.81
110	5.94	7.77	1.83

Transfers to excited states where E_x > 1.8 MeV in In isotopes potentially cause overlaps, but unlikely as they are not single-particle dominated

Literature dσ/dΩ of (d,p) reactions for heavier Sn isotopes: ^{113,115,117}Sn

TABLE I. The energy levels of Sn^{113} from the (d,p) and (d,t) reactions. Listed are the energies, the values of angular momentum transfer, the assigned spins and parity, the absolute cross section for (d,p) taken at the first maximum beyong 9°, the spectroscopic factors and the absolute cross section for (d,t) taken at 45°.

E^* (MeV)	l_n	(d,p) J^π	$(d\sigma/d\Omega)_{max}$ (mb/sr)	$S_{d,p}$	(d,t) E	$d\sigma/d\Omega(45°)$ (mb/sr)
0	0	$\frac{1}{2}+$	4.23	1.16	0	0.699
0.07	4	$\frac{7}{2}+$	0.263	0.31	0.07	0.371
0.41	2	$\frac{5}{2}+$	1.76	0.15	0.39	1.304
0.50	2	$\frac{3}{2}+$	4.75	0.75	0.49	0.314
0.74	5	$11/2^-$	1.20	1.30		
1.01	2	$(\frac{5}{2}+)$	0.216	0.017		
1.56	2	$(\frac{5}{2}+)$	0.730	0.053		
1.82	0	$\frac{1}{2}+$	0.423	0.090		
1.94	1	$(\frac{3}{2}-)$	0.222	0.011		
2.12	3	$(\frac{7}{2}-)$	0.437	0.056		
2.29	3	$(\frac{7}{2}-)$	0.332	0.041		
2.53	3	$(\frac{7}{2}-)$	0.460	0.055		
2.61	3	$(\frac{7}{2}-)$	0.397	0.047		
2.77	3	$(\frac{7}{2}-)$	0.326	0.037		
2.86	3	$(\frac{7}{2}-)$	0.676	0.078		
2.98	3	$(\frac{7}{2}-)$	0.344	0.038		

TABLE II. Energy levels of Sn^{115} from the (d,p) and (d,t) reactions. (See also caption for Table I.)

E^* (MeV)	(d,p) l_n	J^π	$(d\sigma/d\Omega)_{max}$ (mb/sr)	$S_{d,p}$	(d,t) E^* (MeV)	$d\sigma/d\Omega(45°)$ (mb/sr)
0	0	$\frac{1}{2}+$	3.67	0.960	0	1.61
0.49	2	$\frac{3}{2}+$	3.96	0.62	0.48	0.314
0.60	4	$\frac{7}{2}+$	0.209	0.19	0.61	0.368
0.73	5	$\frac{11}{2}-$	0.741	0.77	0.72	0.112
0.98	2	$\frac{5}{2}+$	1.52	0.12	0.98	1.43
1.28	2	$(\frac{5}{2}+)$	0.40	0.029	1.25	0.053
					1.30	0.080
1.63	(2)	$(\frac{5}{2}+)$	0.63	0.044		
1.97	(0)	$\frac{1}{2}+$	0.41	0.082		
2.07	(0)	$\frac{1}{2}+$	0.23	0.045		
2.17	(2)	$(\frac{5}{2}+)$	0.33	0.021		
2.49	(2)	$(\frac{5}{2}+)$	0.35	0.021		
2.77	(1)	$(\frac{3}{2}-)$	0.89	0.050		
2.95	(3)	$(\frac{7}{2}-)$	0.56	0.064		

TABLE III. The energy levels of Sn^{117} from the (d,p) and (d,t) reactions. (See also caption for Table I.)

E^* (MeV)	(d,p) l_n	J^π	$(d\sigma/d\Omega)_{max}$ (mb/sr)	$S_{d,p}$	(d,t) E^* (MeV)	$d\sigma/d\Omega(45°)$ (mb/sr)
0	0	$\frac{1}{2}+$	2.74	0.65	0	2.26
0.16	2	$\frac{3}{2}+$	3.72	0.55	0.16	0.695
0.32	5	$11/2^-$	0.800	0.81	0.31	0.212
0.72	4	$\frac{7}{2}+$	0.166	0.13	0.71	0.306
1.03	2	$\frac{5}{2}+$	0.875	0.061	1.01	1.15
1.19	2	$\frac{5}{2}+$	0.490	0.033	1.18	0.526
1.31	(3)	$(\frac{7}{2}-)$	0.226	0.029		
1.51	(2)	$(\frac{5}{2}+)$	0.315	0.020	1.50	0.173
1.59	(2)	$(\frac{5}{2}+)$	0.098	0.006		
1.67	(2)	$(\frac{5}{2}+)$	0.106	0.007		
1.96	(1+3)	$(\frac{3}{2}-)$	0.040	0.003		
		$(\frac{7}{2}-)$	0.020	0.002		

15-MeV deuterons (~7.5 MeV/u) on stable Sn

Magnitude of dσ/dΩ similar to predictions on lighter isotopes at 8 MeV/u

E. J. Schneid, A. Prakash and B. L. Cohen, Phys. Rev. 156, 1316 (1967)

Cross sections and ISS coverage at 6 MeV/u

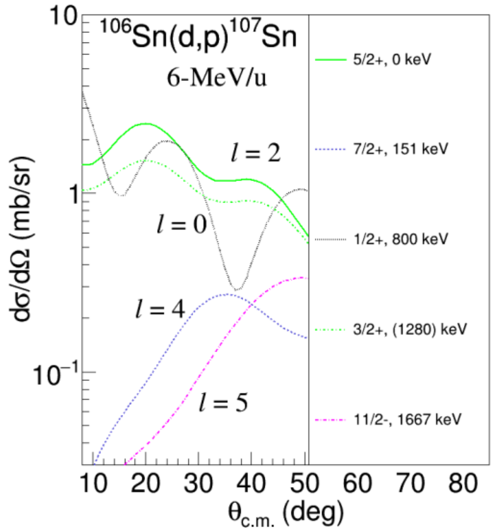

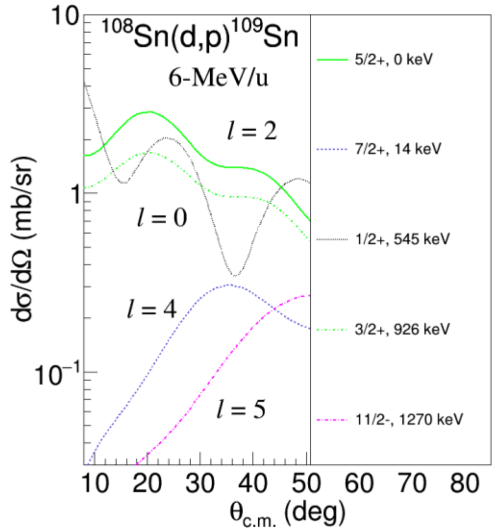

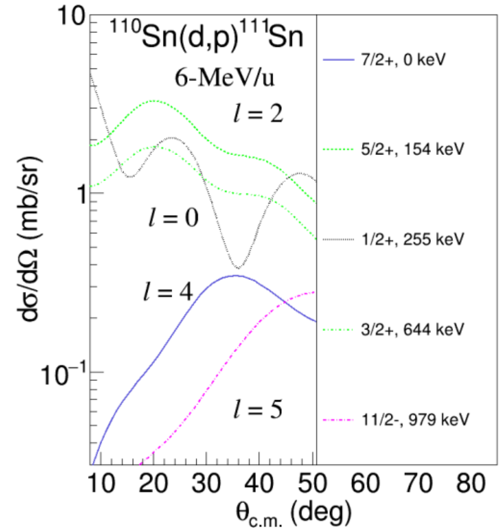

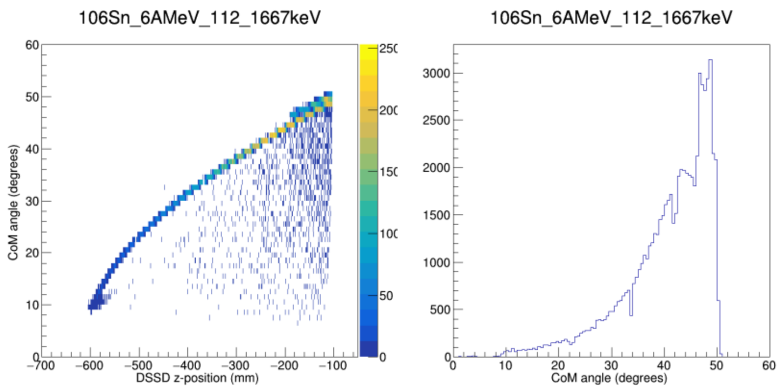

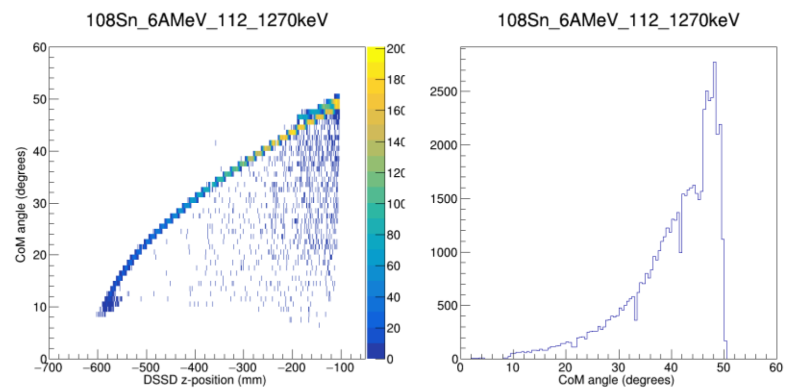

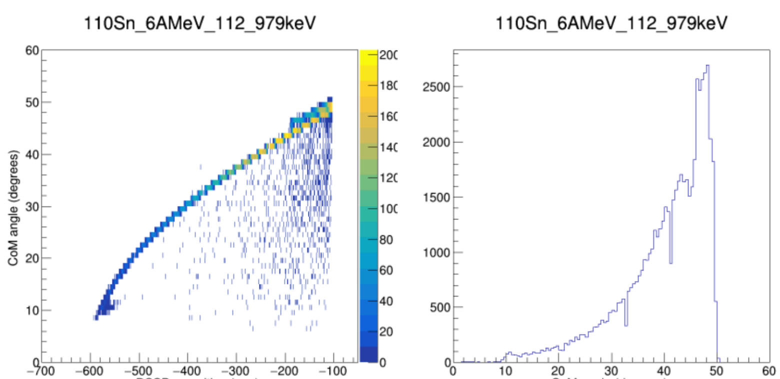

Coverage for (d,p) to 11/2⁻ state
Counts not normalized to cross section

Cross sections and ISS coverage at 8 MeV/u

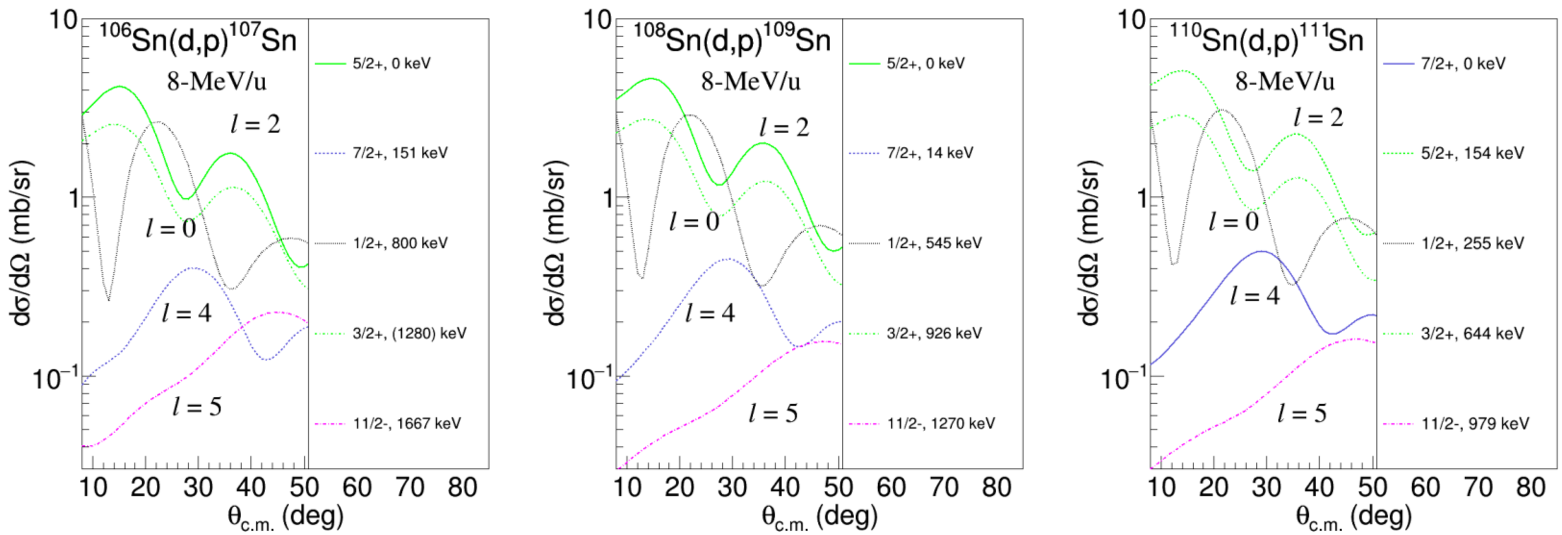

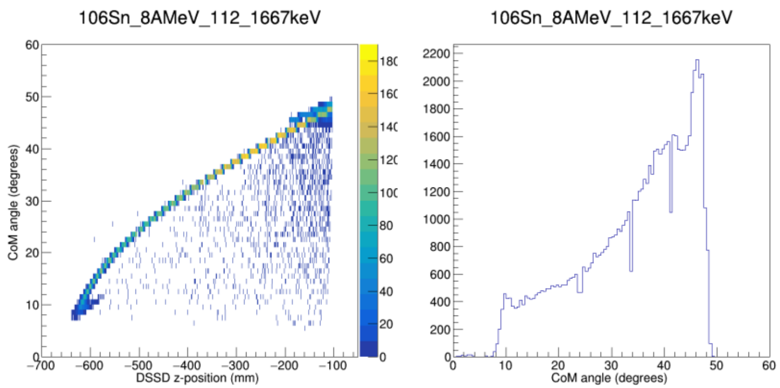

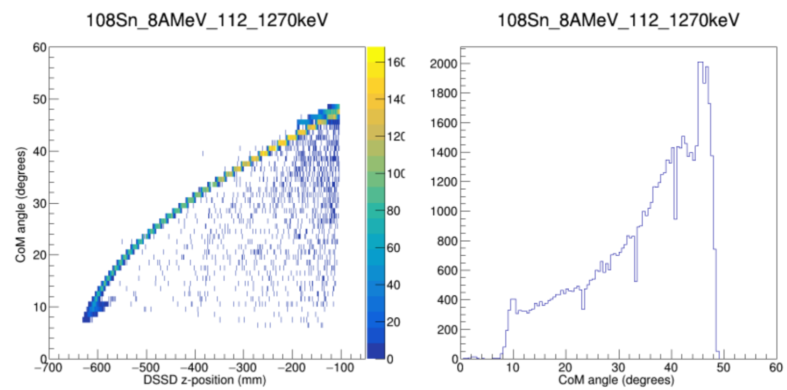

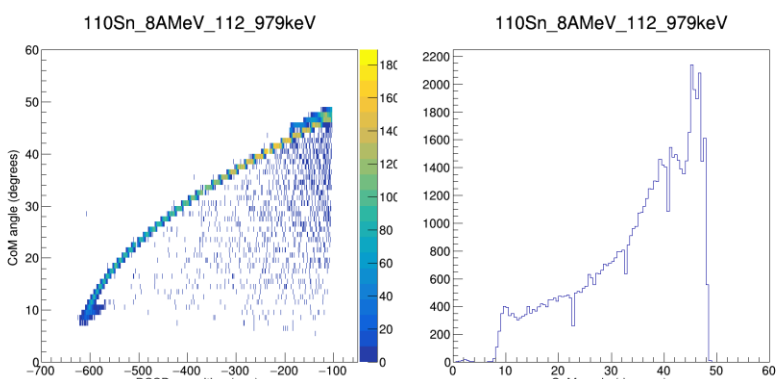

Coverage for (d,p) to $11/2^-$ state
Counts not normalized to cross section

Cross sections and ISS coverage at 10 MeV/u

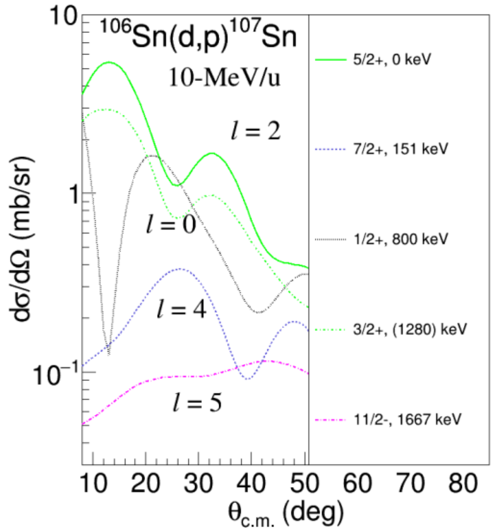

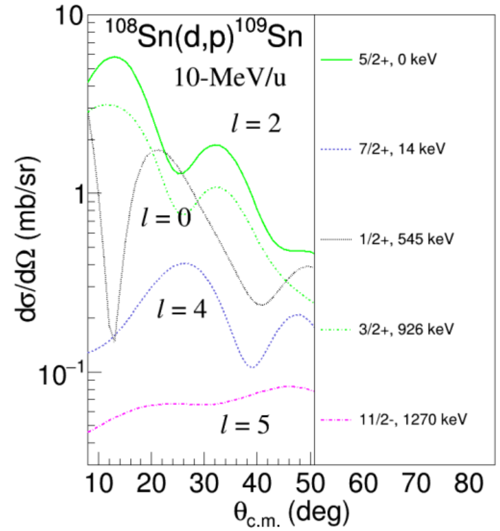

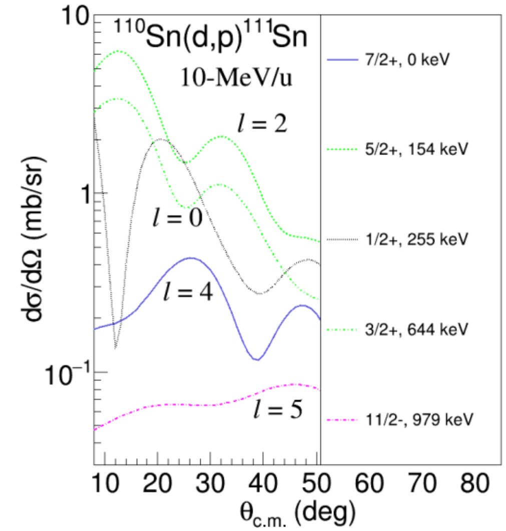

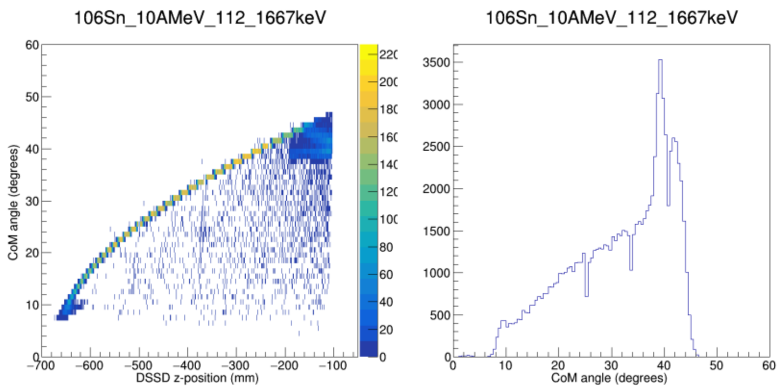

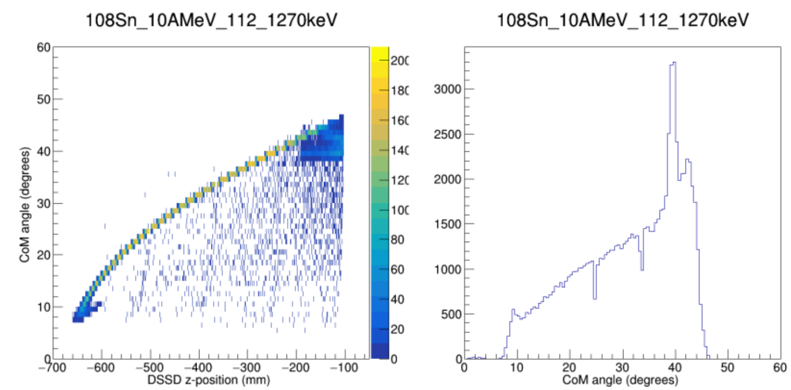

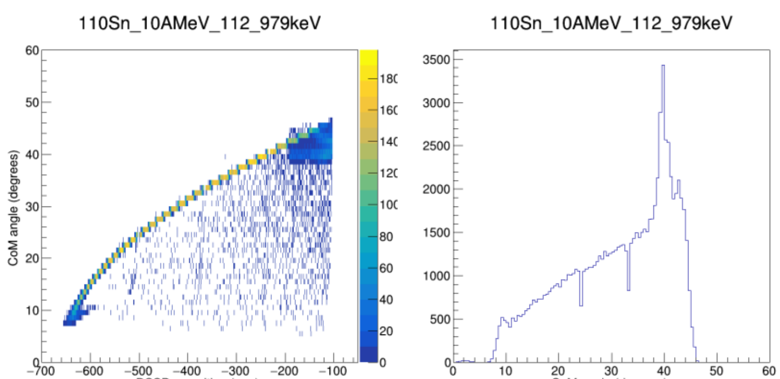

Coverage for (d,p) to 11/2⁻ state
Counts not normalized to cross section

Requirement of ≥100 counts for peak identification

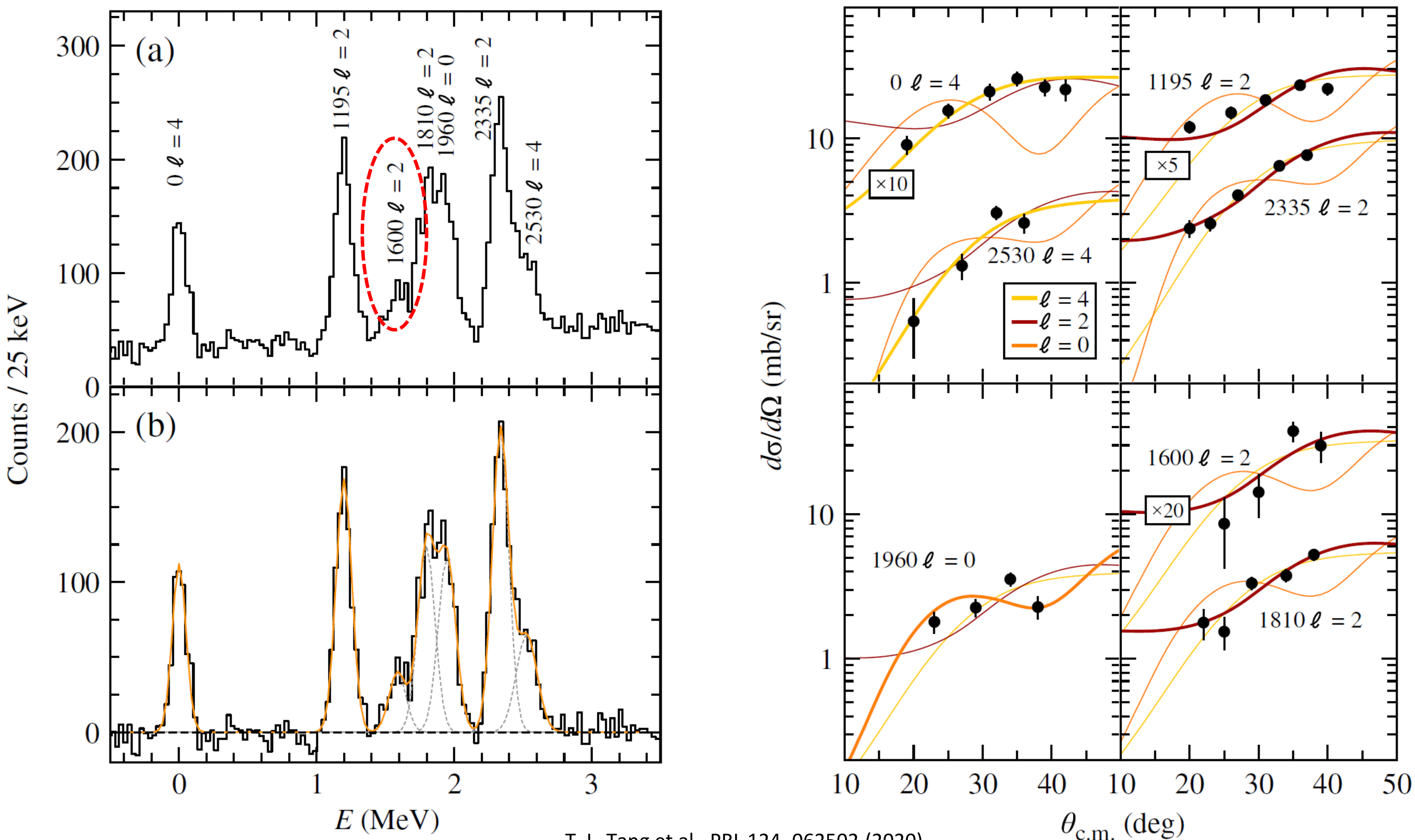

T. L. Tang et al., PRL 124, 062502 (2020)

1600-keV state in ^{207}Hg identified and *S* measured with ca 100 counts, given good energy separation

Summary of proposed (d,p) experiment, IS686

Spectroscopy of single-particle states in $^{107,109,111}Sn$ through (d,p) in inverse kinematics

- Structure evolution towards ^{100}Sn: testing the role of tensor force and deformation
- First (d,p) transfer reactions on light unstable Sn isotopes for J^{π}, E_x and S
- Complementing previously successful Coulex measurements with Miniball

ISOLDE Solenoidal Spectrometer and setup

- 100-keV FWHM energy resolution to distinguish states of interest
- Angular coverage of $8° < \theta_{c.m.} < 49°$ at E_{beam} = 8 MeV/u
- 165-µg/cm^2 CD_2 target, B = 2.5 T

Requested beams and shifts:

Isotope	**Intensity (pps)**	**Energy (MeV/u, ± 0.4-0.5% FWHM)**	**Shifts requested/approved**
^{110}Sn	5×10^5	8.0	12
^{108}Sn	5×10^5	8.0	12
^{106}Sn	1×10^5	8.0	24 (contingent on ^{110}Sn, ^{108}Sn results)

Beam time approved, starting with the heaviest ^{110}Sn and later ^{108}Sn

<u>Experiment in October 2022, stay tuned!</u>